



Current Applications and Advances in Nail Ultrasound Imaging

Ximena Wortsman

Introduction

The nail is one of the main applications of ultrasound in dermatology due to the possibility to observe in detail both the nail plate and the nail bed with high definition [1, 2]. These capabilities allow reducing potential cosmetic sequels secondary to biopsies, besides becoming a powerful diagnostic and monitoring tool for common unguinal conditions [1, 3].

To date, ultrasonography can support the diagnosis in a wide range of unguinal pathologies such as benign and malignant tumors, inflammatory diseases, and location abnormalities [1, 4–6]. Ultrasound can also discriminate between degenerative and inflammatory conditions [7].

During the last decade, ultrasound has significantly improved in the resolution and detection of vascularity. Thus, devices working with high-frequency probes that can vary between 15 and 70 MHz allow discriminating structures that measure 30 μm [8]. Moreover, the new types of vascularity software can detect the slow flow running in submillimeter vessels [8].

The ultrasonographic assessment of the lesional origin (ungual or periungual), size in all axes (mm), exact location (proximal, distal,

central or eccentric, radial or ulnar, medial or lateral), degree of vascularity, and involvement of adjacent tissues can help to select the site and the extent of the incision and have a well-informed presurgical plan [5, 9]. Moreover, for example, in glomus tumors, it has been reported that the patients with presurgical ultrasound examination present a lower rate of recurrence in comparison with cases that did not have previous imaging examinations [10].

The imaging patterns of lesions in several unguinal diseases have been described in a growing list of publications [1, 6, 9, 11–16], which now includes ultrasonographic diagnostic criteria for several of them [17].

Besides the detection of abnormalities in the nail and periungual tissues, ultrasound provides useful data about alterations in the digital skin, joints, tendons, and bony margin [6]. This capability is helpful for the detection of psoriatic arthropathy, which can be relevant in cases that may benefit from more aggressive medications [13].

This chapter aims to review the ultrasonographic advances for nail conditions.

Technical Considerations

This type of examination requires specialized equipment that includes multichannel devices working with linear or compact linear probes that can range in their highest frequency between 15

X. Wortsman (✉)

Institute for Diagnostic Imaging and Research of the Skin and Soft Tissues, Departments of Dermatology, Universidad de Chile and Pontificia Universidad Católica de Chile, Santiago, RM, Chile

and 70 MHz [1, 17, 18]. These high-frequency probes present higher resolution, but their penetration into the tissues is lower; however, most of the machines come with two or three probes that allow moving through a wide range of depth, maintaining a high-definition image through all the layers.

Ideally, the operator of the machine should be trained in imaging and dermatology because there is a gathering of clinical and ultrasonographic information. The possibilities for training in dermatologic ultrasound have substantially increased during the last decade, and besides the significant increment of publications on this topic, there are several annual sessions and courses, some of them under the umbrella of well-known international scientific societies such as the American Institute of Ultrasound in Medicine (AIUM; www.aium.org) or the European Federation of Societies for Ultrasound in Medicine and Biology (EFSUMB; www.efsumb.org) [19].

Examination Technique

The hands and feet need to be in an extended position. For examining the thumbs, it is necessary to use a towel or pad to stabilize the fingers. A copious amount of gel is applied on top of the nail and periungual regions for allowing the passing of the sound waves into the tissues. Then, the operator performs a broad sweep with the probe that includes at least two perpendicular axes. This protocol follows a standardized sequence that starts with grayscale and is followed by a color Doppler and spectral curve analysis. Thus, it is possible to know in advance the presence of hypervascular or hypovascular areas, the type (arterial or venous), and velocity of the flow (cm/sec). Panoramic views, 3D reconstructions, and microvasculature analyses can provide better information or understanding of the characteristics and extent of lesional tissue [1, 17, 18].

Ultrasound Normal Anatomy of the Nail

At 15–18 MHz, the nail plate is observed as a hyperechoic bilaminar structure that presents an outer plate, also called a dorsal plate, and an inner plate, named ventral plate. An anechoic interplate space is located in between the dorsal and ventral plates. However, at 70 MHz, the anechoic interplate space becomes more hyperechoic but less intense than the outer and inner borders of the nail plate [17]. This ultrasonographic appearance has been related to the presence of hard and soft keratin within the nail plate.

The nail bed shows as a hypoechoic space beneath the nail plate that turns to slightly hyperechoic in the proximal part where the matrix region is located [1, 17].

The periungual tissues present the same echostructure of the normal skin, which is a laminar hyperechoic epidermis, and a hyperechoic dermal band, less bright than the epidermis [1, 17, 18].

Arterial flow comes from the digital arteries that supply the nail through the proximal part. Venous flow drains through the digital veins [1, 17, 18].

The bony margin of the distal phalanx presents as a hyperechoic line underneath the distal phalanx [1, 2, 17, 18].

The extensor tendons present a homogeneous fibrillar hyperechoic pattern that shows anisotropy artifact in the distal insertion due to the oblique disposition of the tendons in this part [1, 2, 16].

The joint spaces are slightly perceptible, and occasionally, submillimetric anechoic laminar fluid may be detected [1, 2, 16].

The bony margin of the distal phalanx presents as a hyperechoic line underneath the distal phalanx (Figs. 18.1, 18.2, and 18.3) [1, 3, 17, 18, 20].

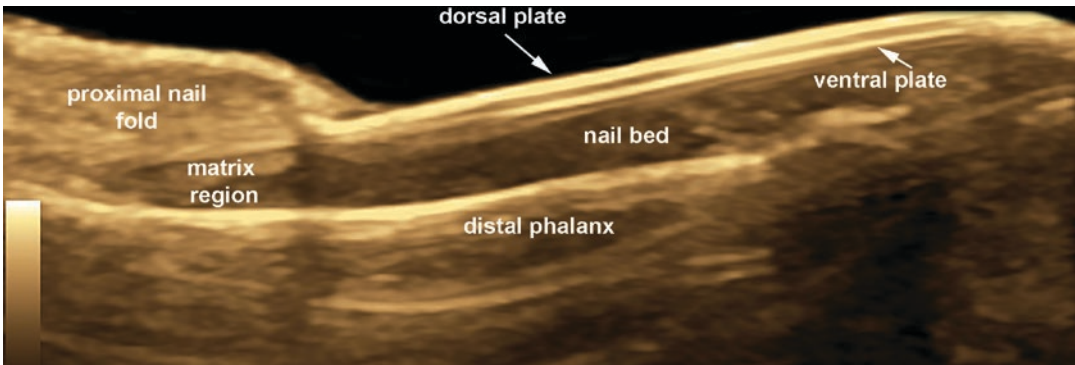


Fig. 18.1 Normal ultrasonographic anatomy of the nail using an 18 MHz maximum frequency probe (longitudinal view)

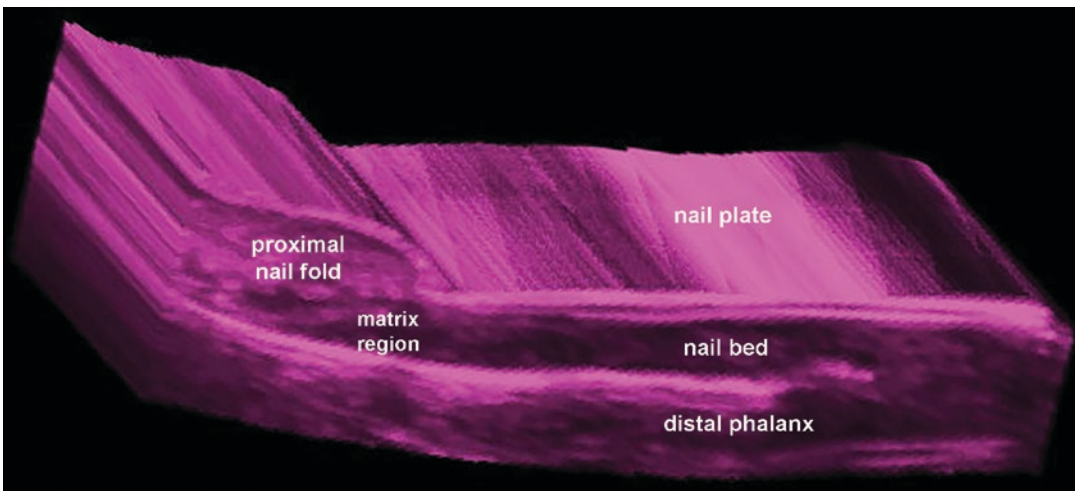


Fig. 18.2 3D normal ultrasound anatomy of the nail (18 MHz)

Main Applications and Advances of Ultrasound of the Nails

Growth and Location Alterations

Onychocryptosis

Ultrasonography can detect the location and size of the fragment of the nail plate embedded in the lateral periungual region. Since many of these

cases are seen in the emergency departments, the ultrasound examination could facilitate the diagnosis and removal of the fragment.

The fragments appear as bilaminar hyperechoic structures within the lateral nail fold. Commonly, there is a hypoechoic thickening or band as well as mild hypervascularity of the periungual dermis due to inflammation (Fig. 18.4) [17, 18, 21].

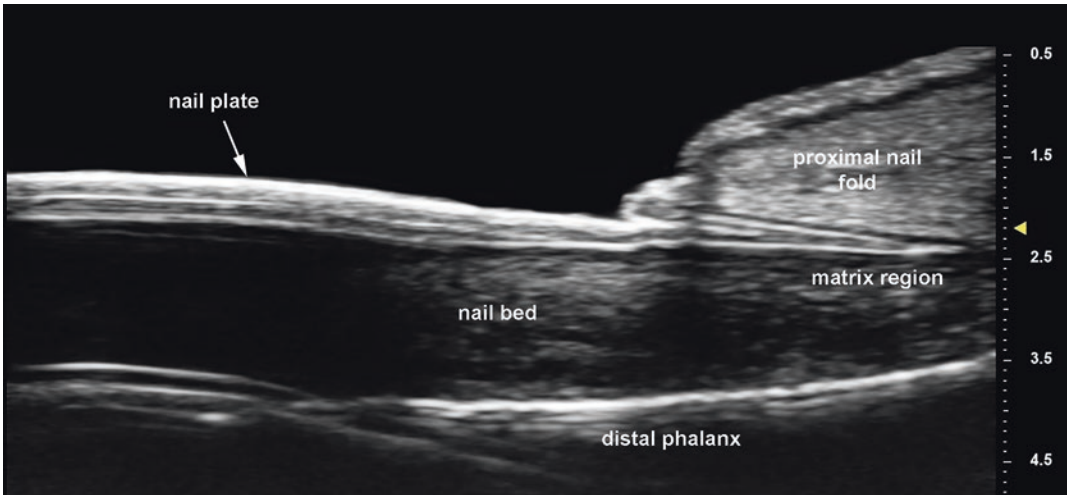


Fig. 18.3 Normal ultrasound anatomy of the nail using a 70 MHz maximum frequency probe (longitudinal view)

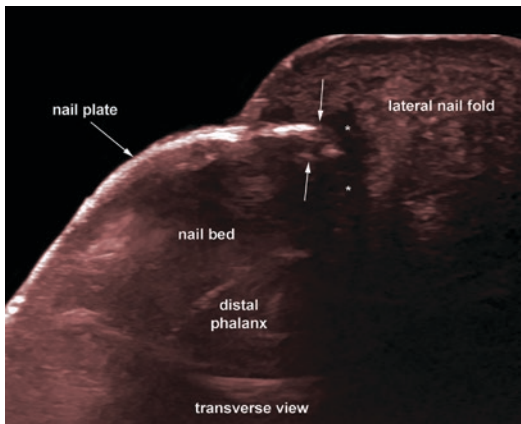


Fig. 18.4 Onychocryptosis. Ultrasound image (18 MHz; transverse view; colored; right big toe) shows hyperechoic and irregular fragment (vertical arrows pointing up and down) embedded in the lateral nail fold. Notice the hypoechoic band (*) in the dermis of the lateral nail fold that corresponds to inflammation

Onychomadesis

The fragmentation of the nail plate is commonly associated with inflammation of the nail bed. On ultrasonography, there are thickening and hypoechogenicity of the nail bed that involves the matrix region. The nail plate is thick and fragmented, and the fragmentation usually starts in the ventral plate (Fig. 18.5) [17, 18, 21].

Retronychia

The posterior embedding of the nail plate can be detected alone or concomitant with onychomadesis. In literature, there are three diagnostic ultrasound criteria for unilateral retronychia: the decrease of the distance between the origin of the plate and the base of the distal phalanx in comparison with the healthy site, the presence of a hypoechoic halo surrounding the origin of the nail plate, and the thickening of the proximal nail fold in the affected side [4, 17]. The ultrasound diagnosis of retronychia needs at least two of these signs, being the halo sign a constant finding [14]. These criteria may help when there is an upward displacement of the nail plate secondary to prominent inflammation. In bilateral retronychia, there are published ultrasound criteria that may help and include, besides the halo sign (constant), a distance between the origin of the nail plate and the base of the distal phalanx ≤ 5.1 mm in big toes and thumbs and/or a difference of ≥ 0.5 mm of this distance between the affected nail (with decreased distance) and the contralateral healthy nail.

Other criteria are a proximal nail fold thickness of ≥ 2.2 mm for male or ≥ 1.9 mm for female patients and/or a proximal nail fold ≥ 0.3 mm thicker in comparison with the contralateral healthy nail (Figs. 18.6, 18.7, and 18.8) [4, 14, 17, 22–24].

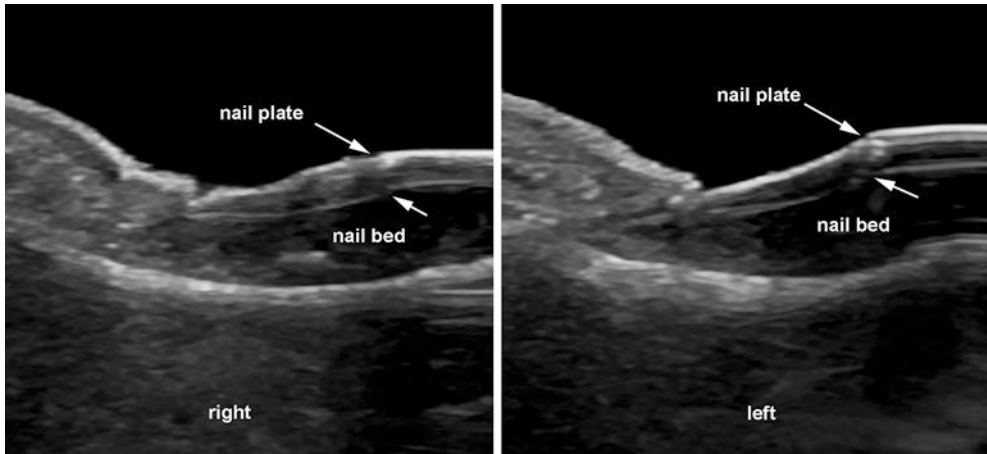


Fig. 18.5 Onychomadesis. Grayscale ultrasound (comparative side-by-side; longitudinal views; big toes) shows fragmentation of the nail bed at both sides, slightly more

prominent on the left. The nail bed is thick and hypochoic, and the nail plates also show increased thickness and irregularities

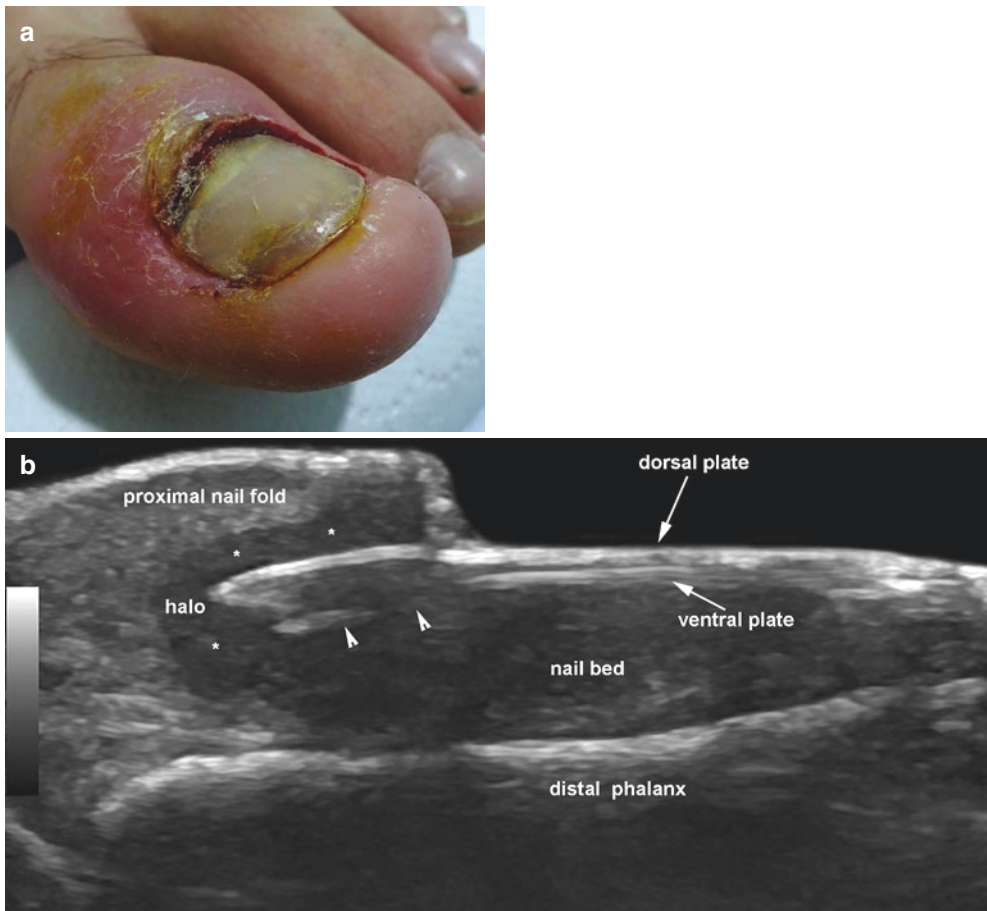


Fig. 18.6 (a, b) Retronychia. (a) Clinical photograph and (b) grayscale ultrasound image (longitudinal view; left big toe; 18 MHz) present embedding of the nail plate into the proximal nail fold. There is a fragmentation of the

ventral plate (arrowheads) and a hypochoic band (*) surrounding the origin of the nail plate. Increased thickness and decreased echogenicity of the dermis at the proximal nail fold seen

Fig. 18.7 Retronychia. Color Doppler ultrasound of the same case of Fig. 18.6 shows increased vascularity at the proximal nail fold that surrounds the origin of the nail plate

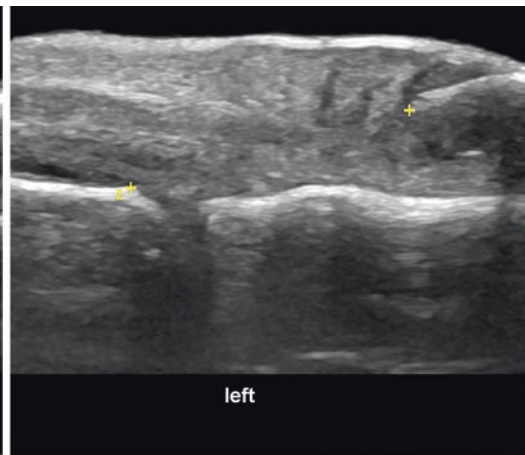
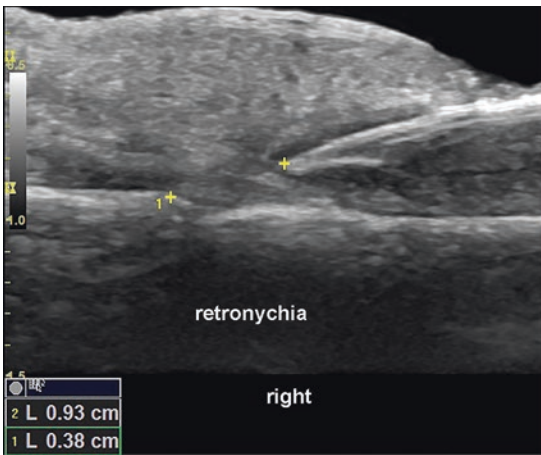
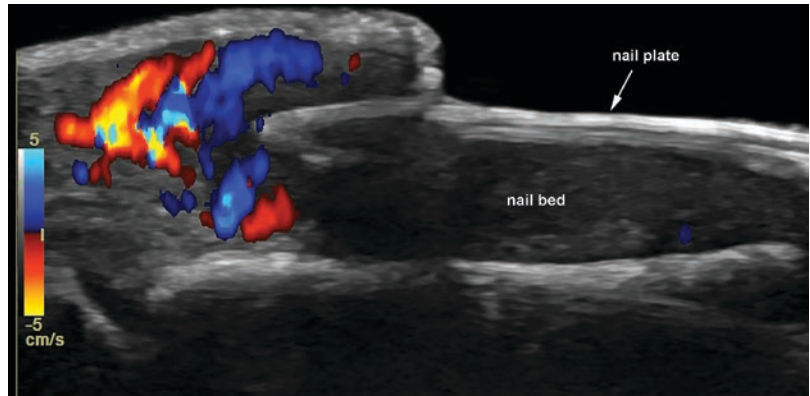


Fig. 18.8 Retronychia. Ultrasound grayscale comparative side-by-side measurement of the distance between the origin of the nail plate and the base of the distal phalanx.

Notice the decreased length of the right side that corresponds to the retronychia (0.38 cm versus 0.93 cm)

Inflammatory Conditions of the Nail

Psoriasis

Ultrasonography can help to diagnose psoriatic onychopathy, and the following signs have been reported: thickening of the nail bed, loss of definition of the ventral plate, hyperechoic deposits in the distal part of the ventral plate, and the presence of thick, irregular, and wavy nail plates [1, 6, 17, 18, 25]. On color Doppler, there is hypovascularity or hypervascularity of the nail bed according to the degree of inflammation (Figs. 18.9 and 18.10) [6, 25]. Moreover, ultrasound can also show the affection of other structures such as the skin, joints, tendons, and

bony margin (Fig. 18.11) [6]. Thus, the assessment of synovitis, tendinopathy, and erosions can support the diagnosis of psoriatic arthropathy, which could imply the management of the patient with more aggressive medications [6, 15, 26–32]. On the other hand, the presence of psoriatic onychopathy seems to be a good predictor of severity and psoriatic arthropathy [33]. The examination is usually performed in all the nails; therefore, the involvement of ≥ 3 nails can be detected earlier, which may help to discriminate better the patients with more severe forms of presentations [34]. Regarding the ultrasonographic differential diagnosis between psoriasis and onychomycosis, there is

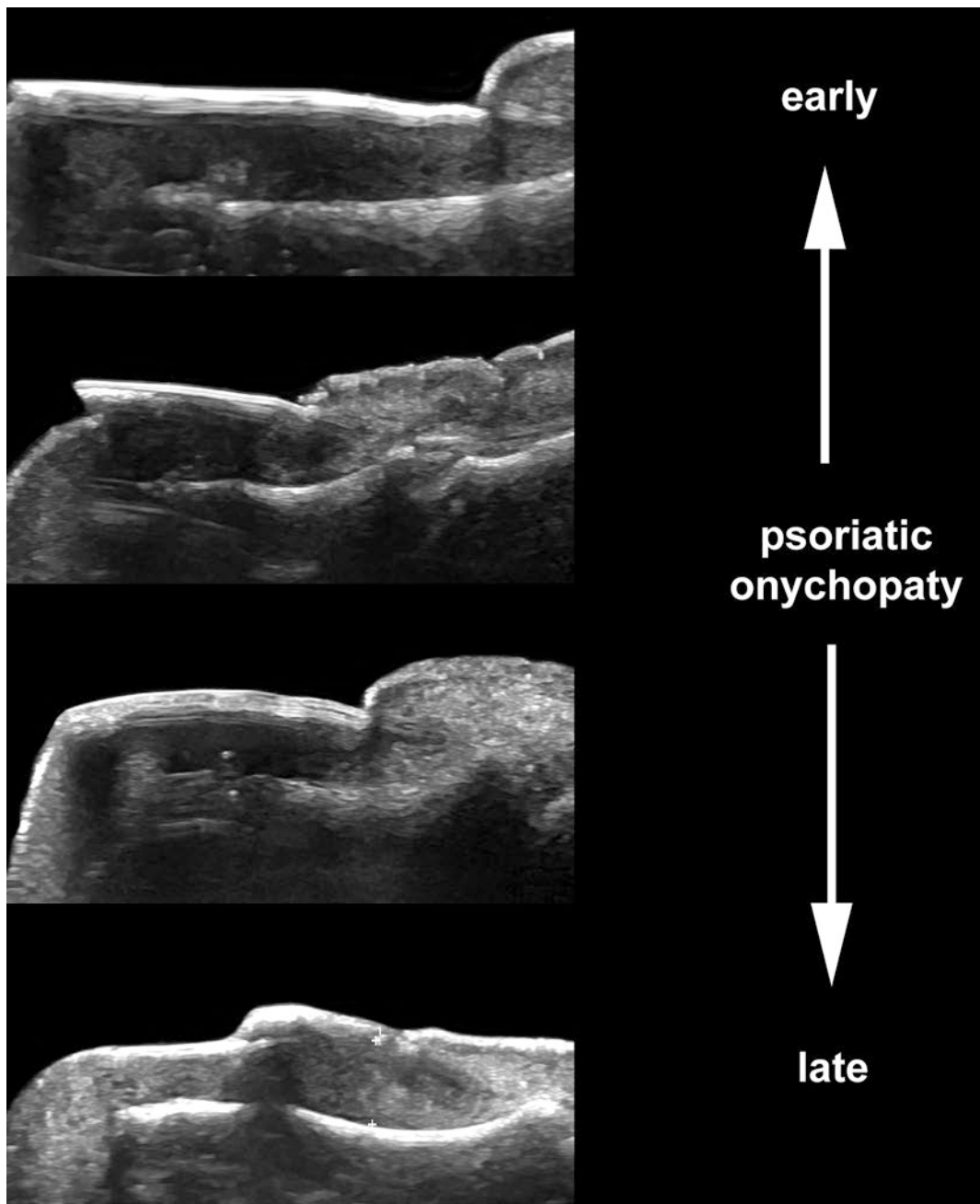


Fig. 18.9 Psoriasis. Ultrasound grading of severity in psoriatic onychopathy

little information in the literature [29] and commonly, these two entities are associated [35]; therefore, the discrimination could be complicated. Furthermore, the patients go to the ultrasound examination after the fungus test is

negative and/or they have received antimycotic treatment for several months. In our experience, onychomycosis tends to affect the superficial nail bed and the nail plate, in contrast to psoriasis that affects the whole thickness of the nail

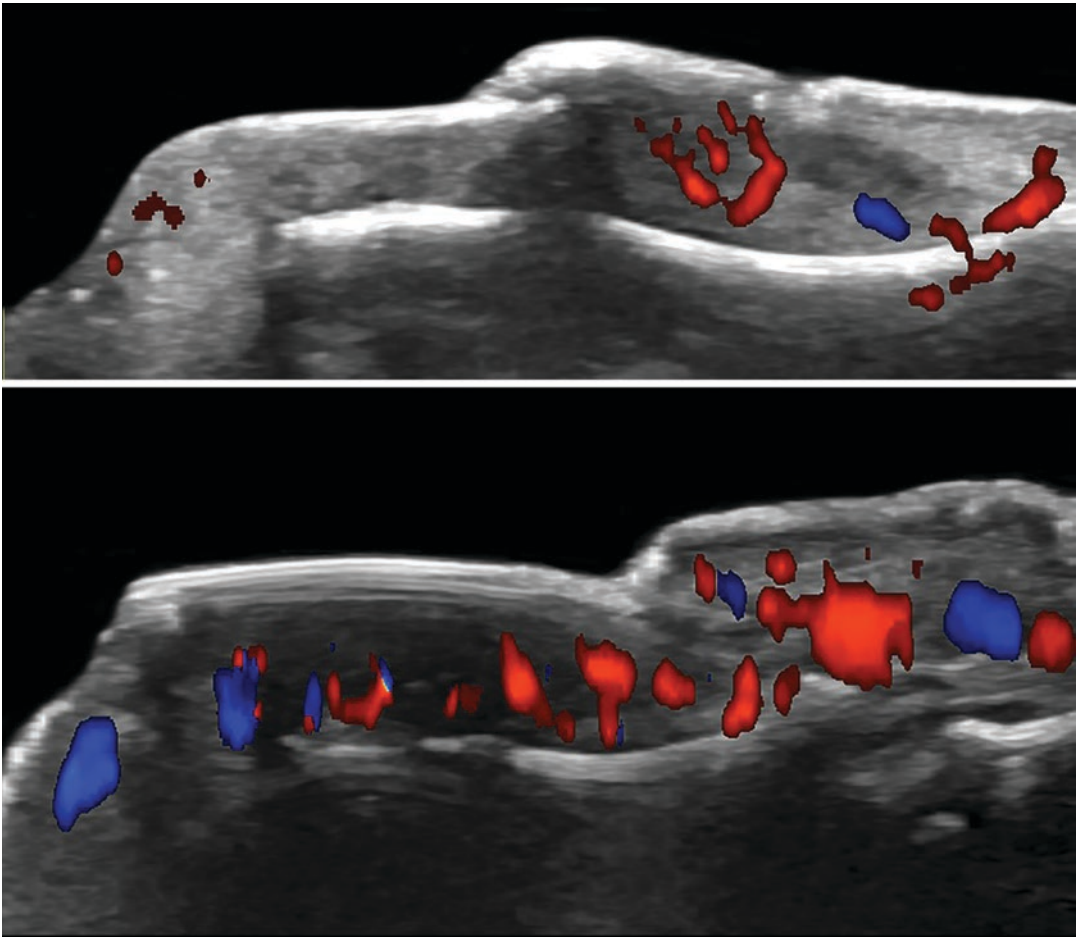


Fig. 18.10 Psoriasis. Color Doppler ultrasound grading of vascularity in psoriatic onychopathy

bed, besides the nail plate [6, 13, 15, 17, 18, 25, 26, 28–30]. Ultrasound has been additionally used for monitoring biologic drugs in psoriatic onychopathy [36].

Morphea/Scleroderma

Increased thickness and hypoechogenicity of the nail bed with an upward displacement of the nail plate are common findings in morphea or scleroderma [17, 37]. On color Doppler, hypovascularity of the nail bed is frequent, particularly in patients with Raynaud syndrome. Decreased echogenicity of the periungual dermis and increased echogenicity of the subcutis of the fingers with loss of the dermal-hypodermal borders are also detected (Fig. 18.12) [17, 18].

Fluid Collections

Anechoic laminar subungual collections are possible to detect in the nail bed. In cases with purulent material, the content may be hypoechoic. On color Doppler, there is hypovascularity or hypervascularity of the nail bed according to the degree of inflammation (Fig. 18.13) [17, 18, 21].

Median Canaliform Dystrophy

The thinning of the proximal and central part of the nail bed that includes the matrix region is a common finding in this condition. Central irregularities and loss of the bilaminar structure of the nail are additional findings. On color Doppler, these cases tend to present a hypovascular nail bed to scarring (Fig. 18.14) [17, 18].

Fig. 18.11 Ultrasonographic alterations of tissues in psoriasis. Active psoriatic changes (color Doppler and grayscale) in the skin (cutaneous plaque), nail (onychopathy), entheses (tendinopathy), joint (synovitis), and bone (erosion marked with an arrow)

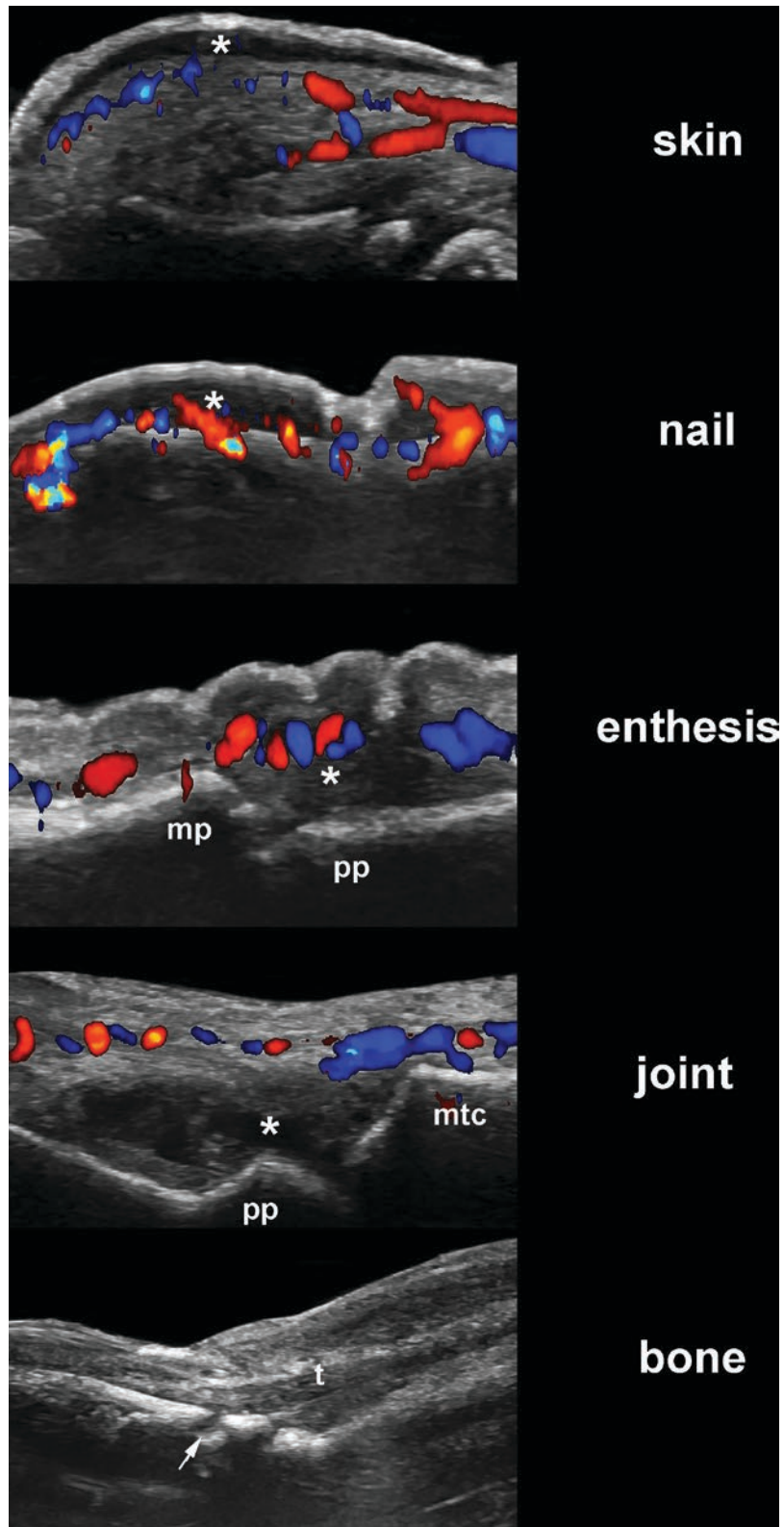


Fig. 18.12 (a, b) Morphea. (a) Grayscale and (b) color Doppler ultrasound demonstrate slightly increased thickness and hypovascularity of the nail bed (b)

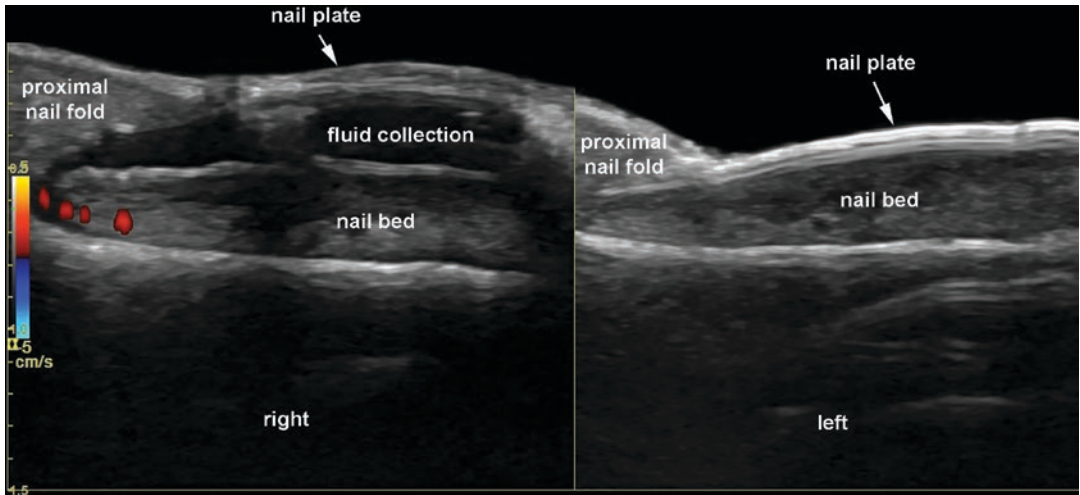
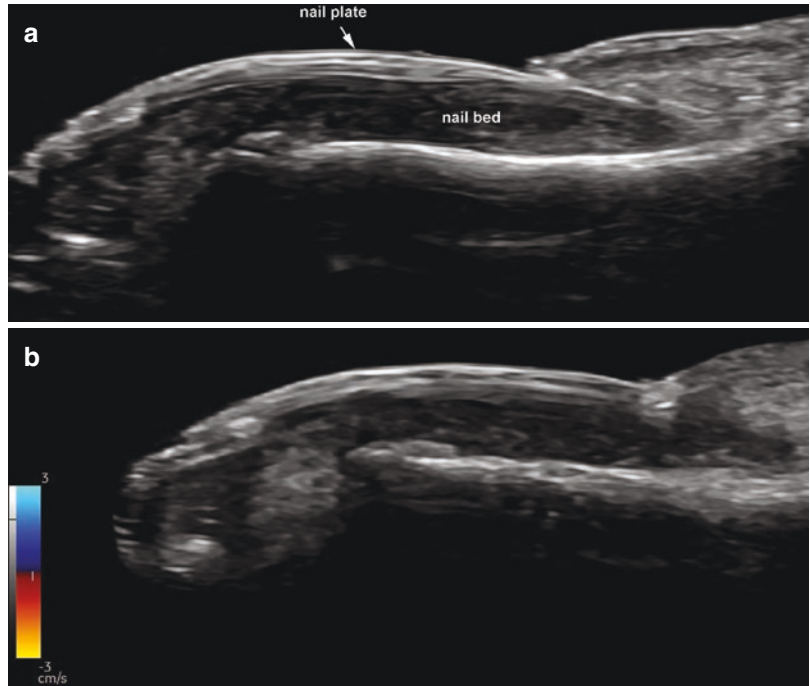


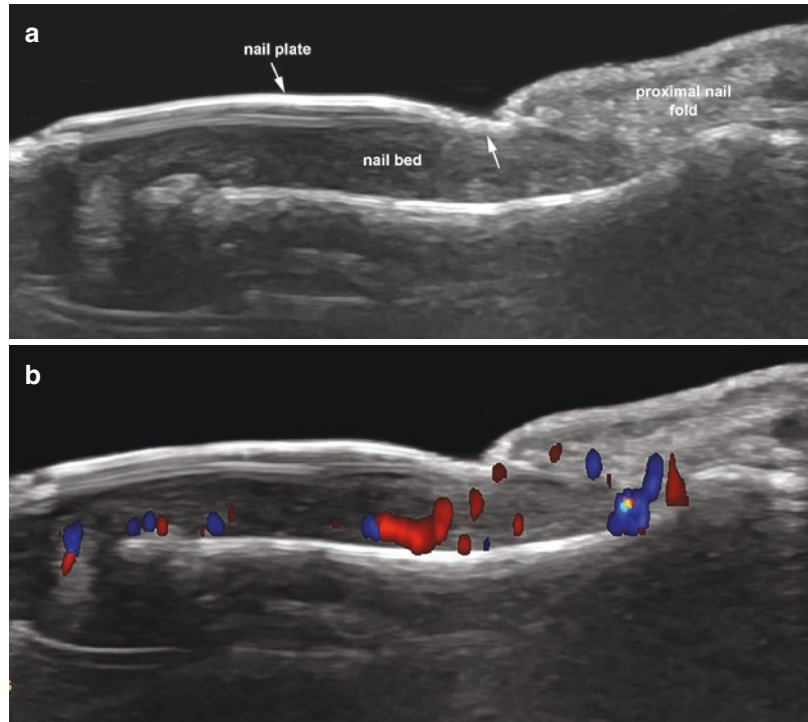
Fig. 18.13 Subungual fluid collection. Color Doppler ultrasound comparative side-by-side longitudinal view shows an anechoic band that corresponds to a fluid collection in between the nail plate and the nail bed at the right side

Subungual Warts

These are secondary to human papillomavirus infections and commonly affect the periungual and unguinal regions [38, 39]. On ultrasound, they present similar morphology to warts on other

locations of the body, which includes a fusiform shape and hypoechoic subungual and/or periungual structure with irregularities of the nail plate (Fig. 18.15 and 18.16) [17, 18].

Fig. 18.14 (a, b) Median canalicular dystrophy. (a) Grayscale ultrasound demonstrates heterogeneous echogenicity and thickening of the proximal part of the nail bed with irregularities of the proximal part of the nail plate (central part). (b) Color Doppler ultrasound presents hypervascularity of the proximal nail bed and the dermis of the proximal nail fold



Benign Tumors and Pseudotumors

We will review the most common requests for an ultrasound examination. For academic purposes, the conditions are divided according to their main origin into ungual and periungual [5, 17, 18].

Ungual Origin

These are separated according to nature in solid and cystic.

Solid

Glomus Tumors

These are tumors derived from the neuromyoarterial plexus, and their most common location is the nail. Almost 70% of cases are located at the proximal part of the nail bed (central or eccentric), and the remaining percentage is reported to show a distal location. On ultrasound, the most common form of presentation is a well-defined oval-shaped nodule in the nail bed that generates scalloping of the bony margin of the distal phalanx [5, 10, 11]. Occasionally, cases with

multiple glomus tumors have been described in the literature [40]. On color Doppler, they tend to be hypervascular with slow-flow arterial vessels; however, some rare variants such as glomangiomyomas may show hypovascularity (Fig. 18.17) [5, 10, 11, 17, 18].

Fibromatous Tumors

These comprise a heterogeneous group of benign entities that can present as subungual or periungual eccentric hypoechoic structures or bands. Subungual fibromas tend to affect the lateral nail fold and present as ill-defined or lobulated areas that compress the nail plate and remodel the bony margin. Periungual fibromas commonly present as well-defined band-like structures and involve the proximal nail fold where they contact and extrinsically compress the origin of the nail plate. Fibrokeratomas can show an irregular hyperechoic area in their distal part due to the presence of hyperkeratosis. On color Doppler, fibromas are commonly hypovascular. However, some variants, such as angiofibromas, can be associated with prominent vessels (Figs. 18.18 and 18.19) [5, 17, 18].

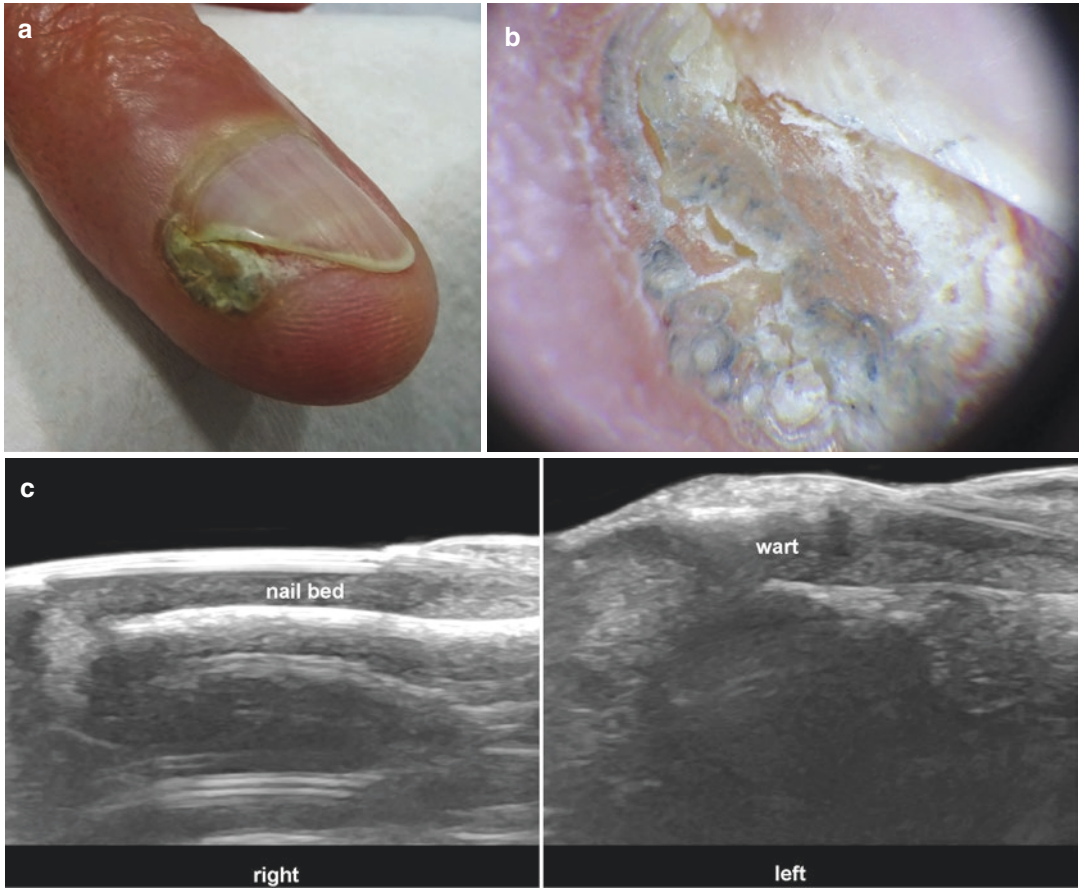


Fig. 18.15 (a–c) Subungual wart. (a) Clinical, (b) dermoscopy, and (c) ultrasound (grayscale, side-by-side comparative images; right versus left ring fingers) present

at the left side a hypoechoic and fusiform thickening of the nail bed with irregular thickening of the nail plate (wart region)

Onychomatricoma

This tumor is derived from the nail matrix, and its ultrasound morphology is characterized as an ill-defined, eccentric, and proximal hypoechoic structure with hyperechoic lines that protrude into the nail plate. On color Doppler, its vascularity can be variable, which can go from hypovascular to an intermediate degree of vascularity (Fig. 18.20) [5, 17, 18, 41].

Granuloma

This pseudotumor is usually associated with chronic inflammation and appears on ultrasound as an ill-defined thickening and hypoechogenicity of the nail bed that displace the nail plate upward. On color Doppler, their vascularity is variable

and can go from hypovascular to hypervascular (telangiectatic or pyogenic variant).

Some telangiectatic subungual granulomas may mimic amelanotic melanoma due to their intense hypervascularity. These telangiectatic

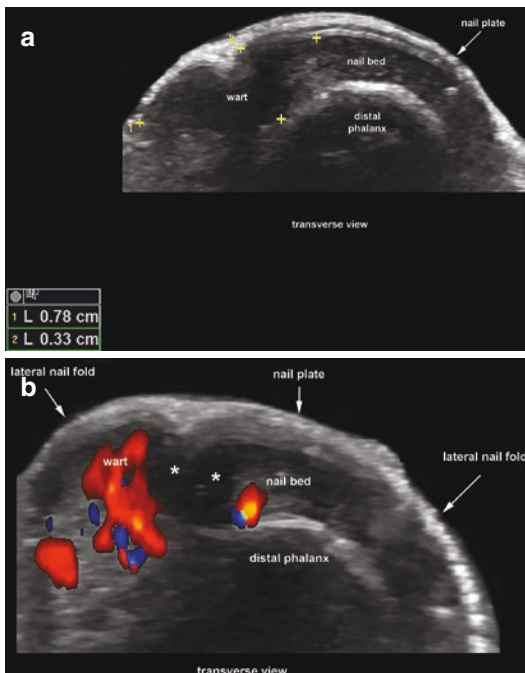


Fig. 18.16 (a, b) Subungual and periungual wart. (a) Grayscale and (b) color Doppler ultrasound (transverse view; left ring finger) of the same case of Fig. 18.15 demonstrate hypoechoic fusiform thickening of the nail bed and periungual dermis of the lateral nail fold (radial border). Notice the subungual and dermal hypervascularity in b

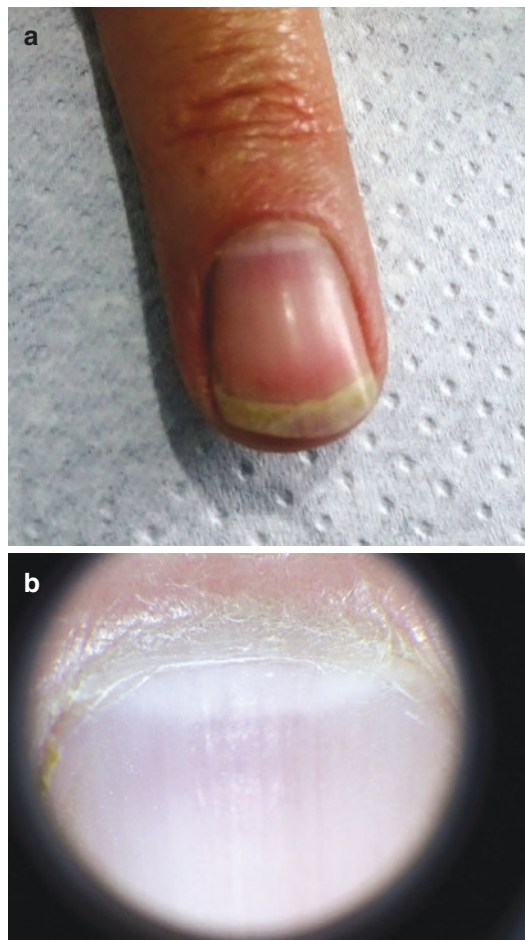


Fig. 18.17 (a–f) Glomus tumor (left ring finger). (a) Clinical photograph. (b) Dermoscopy image. (c, d, and f) Ultrasonographic longitudinal views (c, grayscale ultrasound at 18 MHz; d, color Doppler ultrasound at 18 MHz; e, grayscale side-by-side comparative images; and f, color Doppler ultrasound at 70 MHz). Notice the well-defined, oval-shaped hypoechoic structure (*, between markers) located in the proximal part of the nail bed. There is hypervascularity within the nodule in d and f

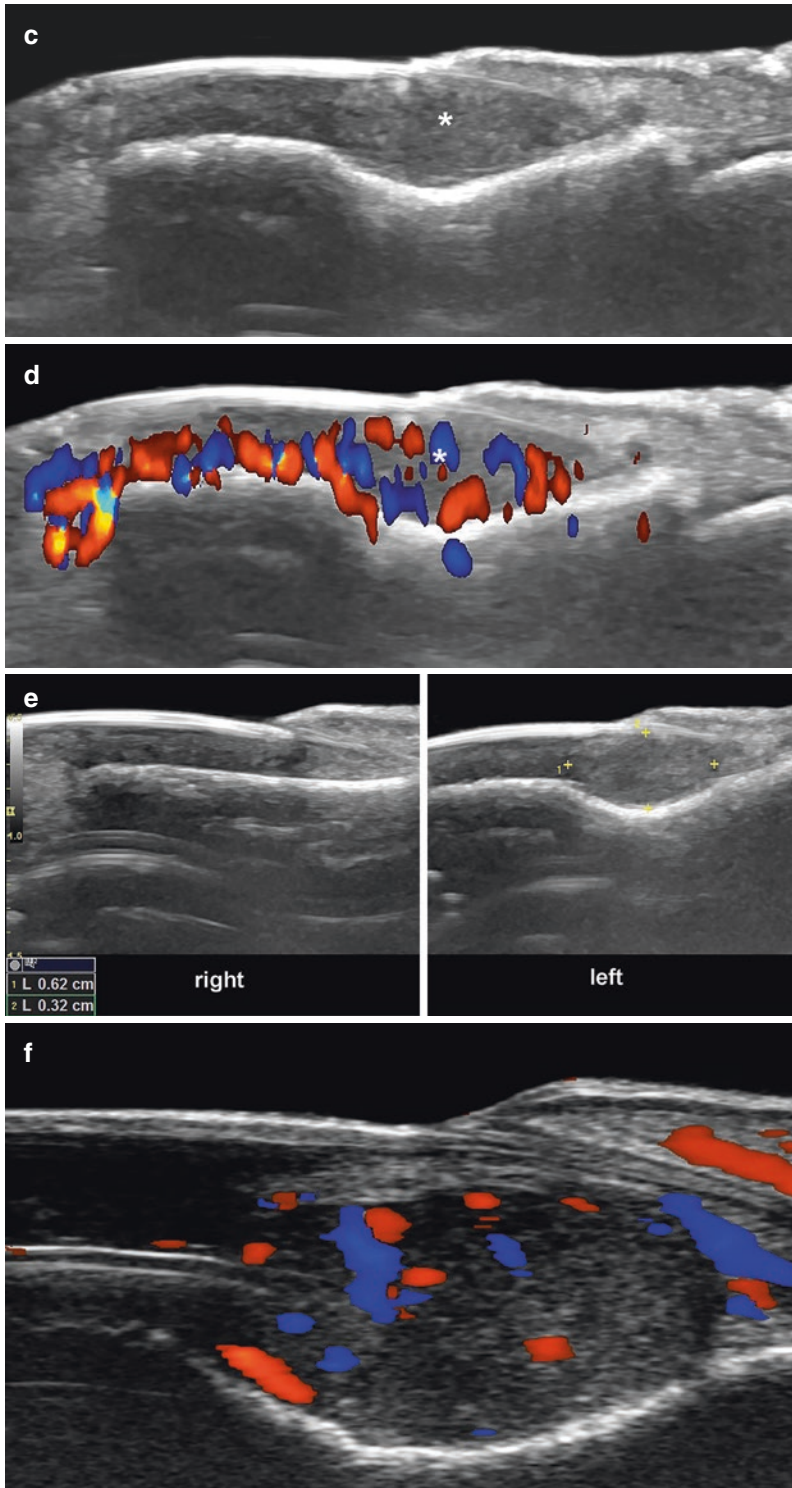
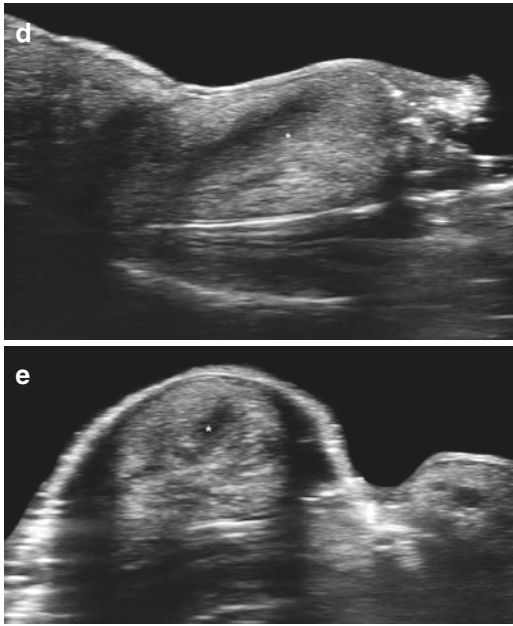


Fig. 18.17 (continued)



Fig. 18.18 (a–e) Periungual fibroma (left big toe). (a) Clinical photograph. (b–e) Ultrasound images (b–d, longitudinal views; e, transverse view; b, d, and e, grayscale; and c, color Doppler) present band-like hypoechoic struc-

ture (*) at the proximal nail fold compressing the proximal part of the nail plate and attached to the proximal part of the nail bed. Notice the hypovascularity of the tumor in c



granulomas can also affect the proximal nail fold (Fig. 18.21) [5, 17, 18].

**Cystic
Mucous Cysts**

These are originated by degeneration of the collagen of the nail bed. On ultrasound, they show as oval- or round-shaped anechoic subungual structures that displace the nail plate upward and may present internal echoes. Mucous cysts commonly affect the nail matrix region and generate irregularities of the nail plate and do not connect with the interphalangeal joint. On color Doppler these cysts are avascular (Fig. 18.22) [17, 18].

**Periungual Origin
Subungual Exostoses**

These benign bony outgrowths derived from the distal phalanx and protrude into the nail bed. On ultrasound, they appear as hyperechoic irregular

Fig. 18.18 (continued)

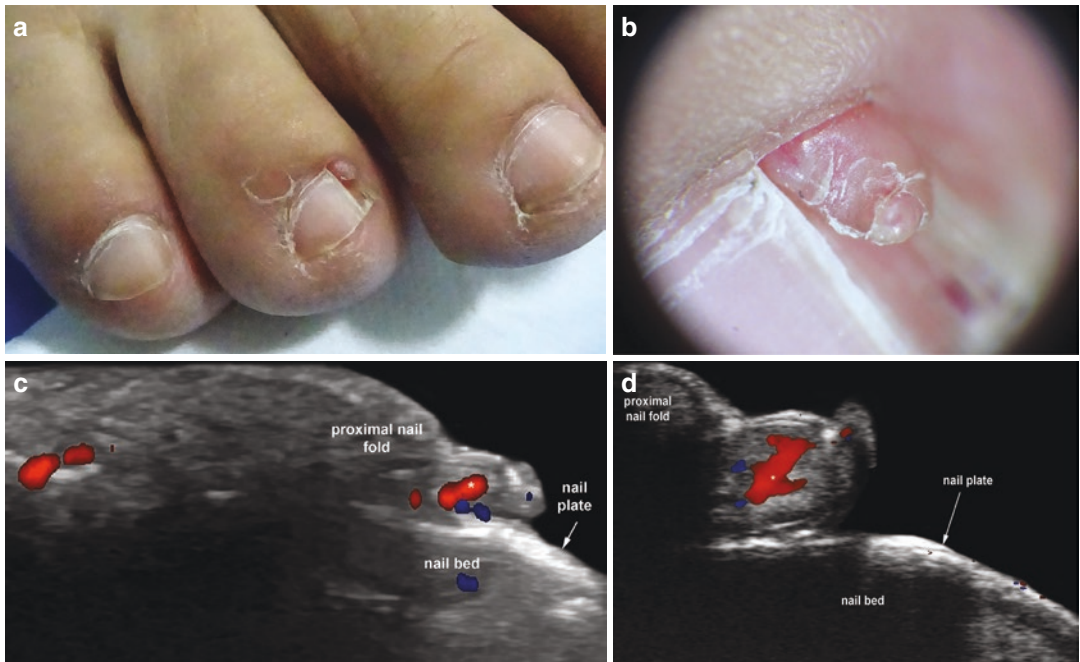


Fig. 18.19 (a–d) Periungual angiofibroma (right fourth toe). (a) Clinical photograph. (b) Dermoscopy. (c and d) Color Doppler ultrasound images (c, at 18 MHz; d, at

70 MHz) show hypoechoic band-like structure (*) with central vascular pedicle (in colors)

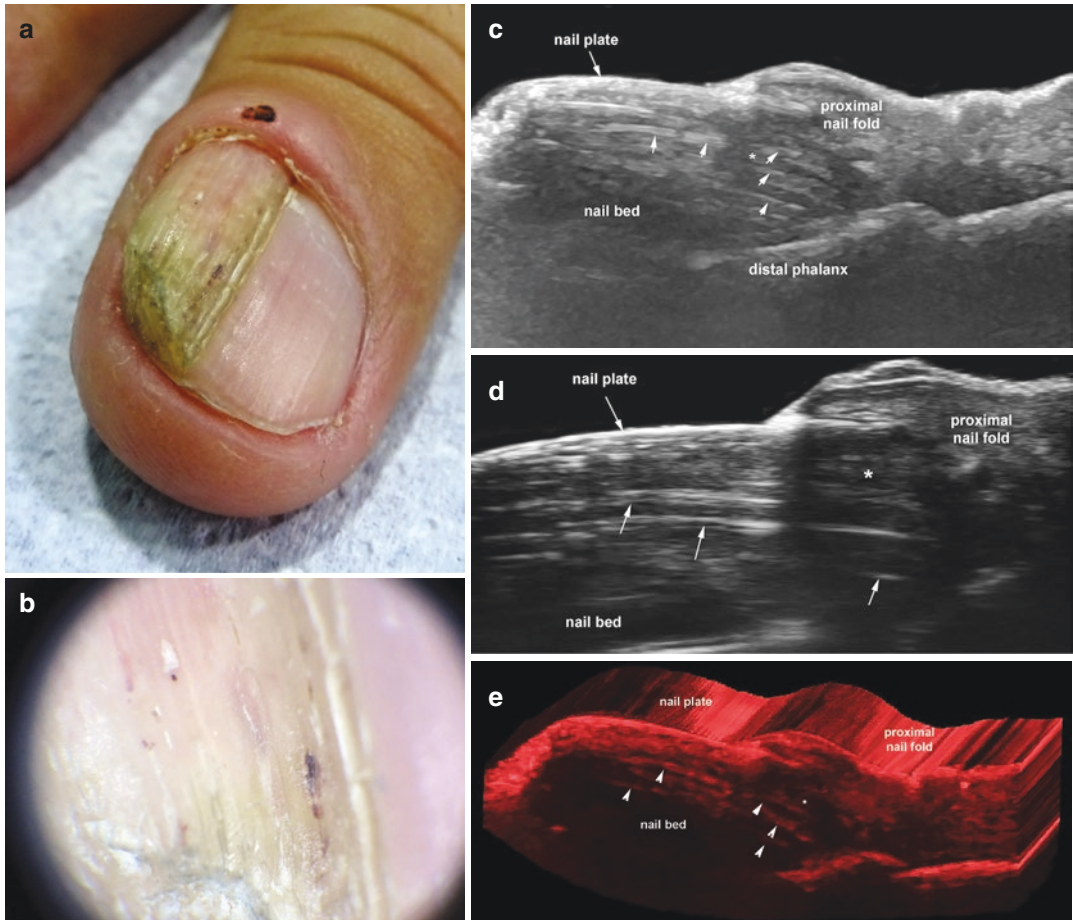


Fig. 18.20 (a–e) Onychomatricoma (left middle finger). (a) Clinical photograph. (b) Dermoscopy. (c, d and e) Ultrasound images (longitudinal views; c, 18 MHz, d, 70 MHz, and e, 3D reconstruction at 18 MHz) show

hypoechoic subungual structure (*) in the radial aspect with hyperechoic lines (arrows and arrowheads) that protrude into the nail plate

bands that generate posterior acoustic shadowing due to the calcium of the bone. Osteochondromas may also present as a hyperechoic band with posterior acoustic shadowing, and the cartilaginous part of the tumor usually shows a hypoechoic cap. The nail bed is commonly thick and hypoechoic because it presents a secondary inflammatory and granulomatous reaction. According to the

degree of affection of the nail matrix, there is a variable amount of thickening and irregularities in the nail plate (Fig. 18.23) [17, 18].

Synovial or Myxoid Cysts

These pseudotumors are originated in the distal interphalangeal joint, and its synovium and fluid extend into the proximal nail bed. Occasionally

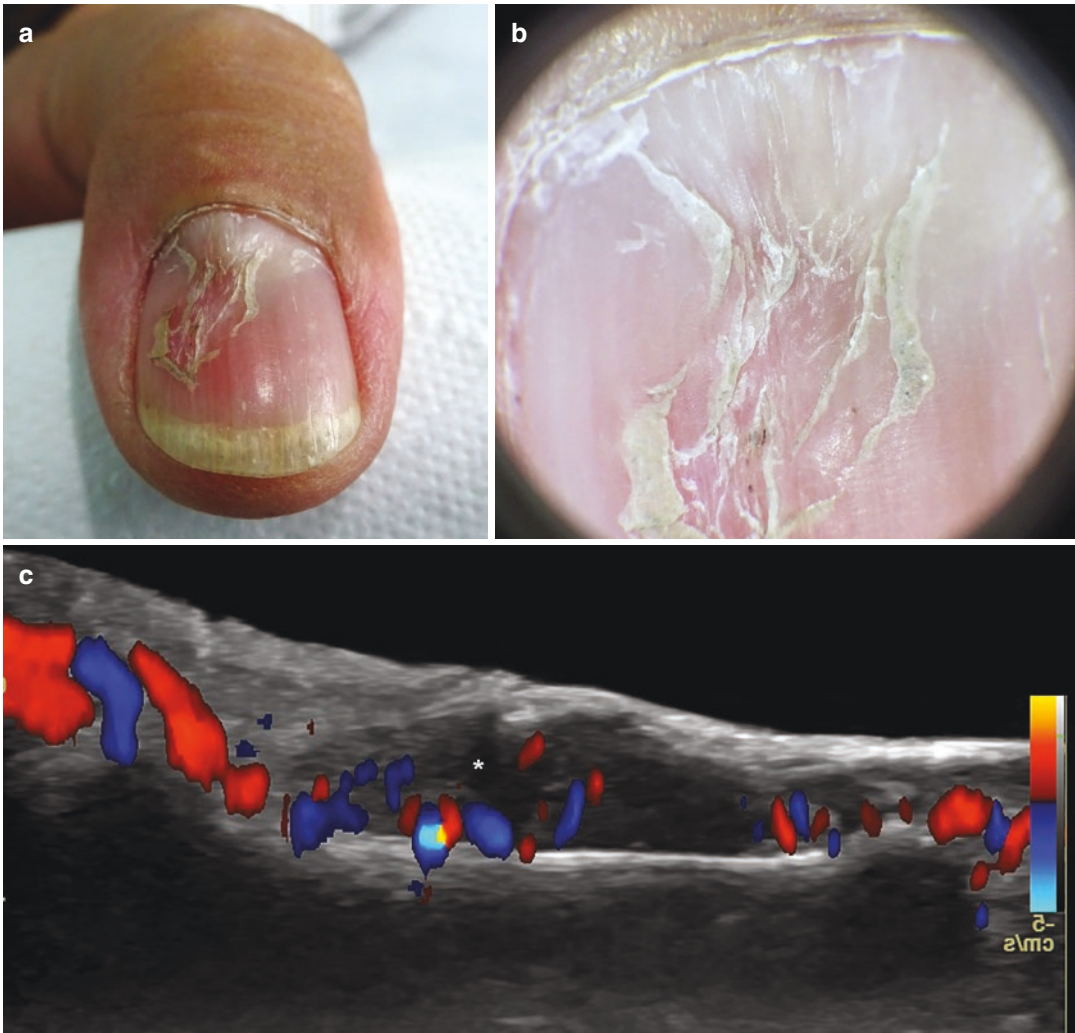


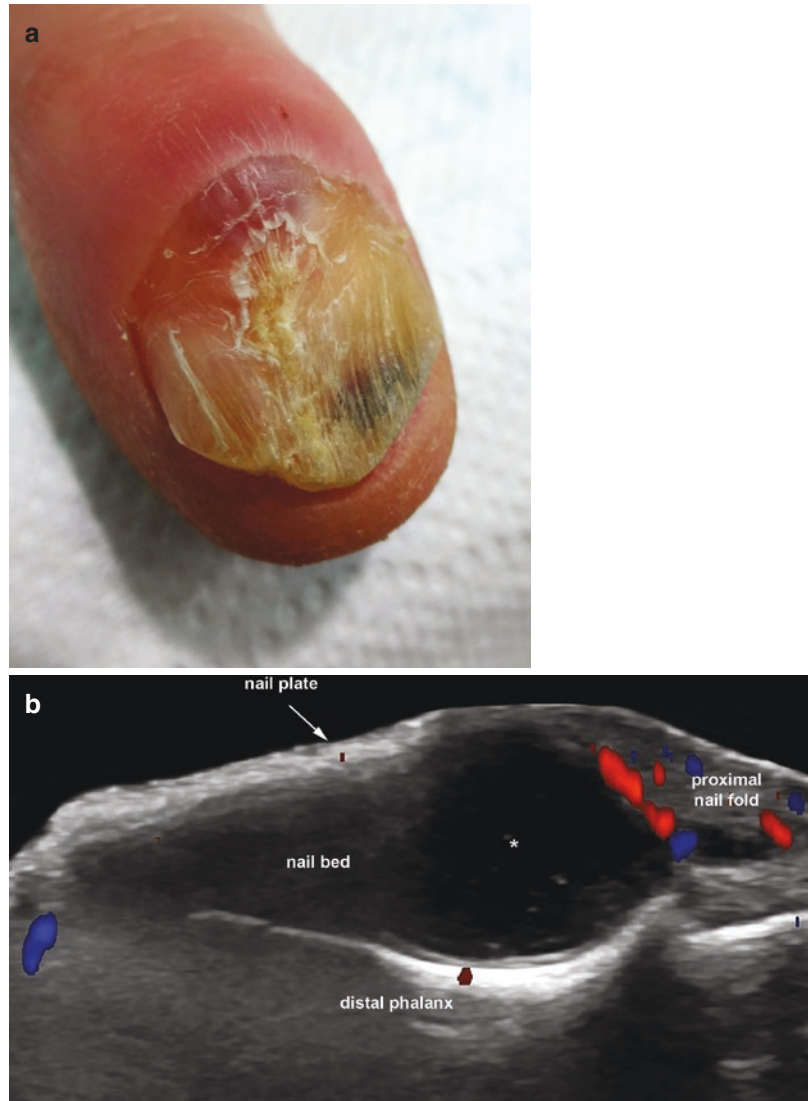
Fig. 18.21 (a–c) Subungual granuloma (left thumb). (a) Clinical photograph. (b) Dermoscopy. (c) Color Doppler ultrasound (longitudinal view) demonstrates hypoechoic thickening (*) and mild hypervascularity of the proximal

part of the nail bed that involves the matrix region and displaces the nail plate upward. Notice the increased thickness and irregularities of the nail plate

these cystic lesions can protrude into the nail bed. On ultrasound, they show as a well-defined oval-shaped structure with internal echoes and connected with the joint through a thin duct. Sometimes there are two or more connections to the joint, and commonly, there are degenerative signs in the distal interphalangeal joint (DIP) with anechoic fluid, prominent hypoechoic synovium, and hyperechoic periarticular osteo-

phytes. Ultrasound can support the diagnosis and locate the site of the connection to the DIP. Due to the extrinsic compression of the nail plate, there is a distal concavity of the bilaminar ungual structure that follows the axis of the cyst. On color Doppler, these cysts are avascular; however, hypervascularity of the proximal nail fold can be detected according to the level of inflammation (Fig. 18.24) [17, 18].

Fig. 18.22 Mucous cyst (**a, b**) (right index). (**a**) Clinical image. (**b**) Color Doppler ultrasound (longitudinal view) shows an oval-shaped, anechoic, and avascular structure with internal echoes in the proximal part of the nail bed. This structure produces a posterior acoustic reinforcement artifact typical of fluid-filled conditions and involves the matrix region. There are vessels (in colors) in the proximal nail fold at the periphery of the cyst. No connection was found between the cyst and the distal interphalangeal joint



Malignant Tumors of the Nail

Squamous Cell Carcinomas

These malignant tumors appear on ultrasound as ill-defined and eccentric hypoechoic and heterogeneous structures that commonly erode the nail plate and the bony margin of the distal phalanx as well as affect the lateral nail fold. On color

Doppler, there is hypervascularity of the nail bed in the site of the tumor (Fig. 18.25) [17, 18].

Subungual Melanomas

The detection of pigments such as melanin is one of the limitations of ultrasound; nevertheless, it is possible to detect a mass-like structure [42]. According to the degree of invasion, subungual

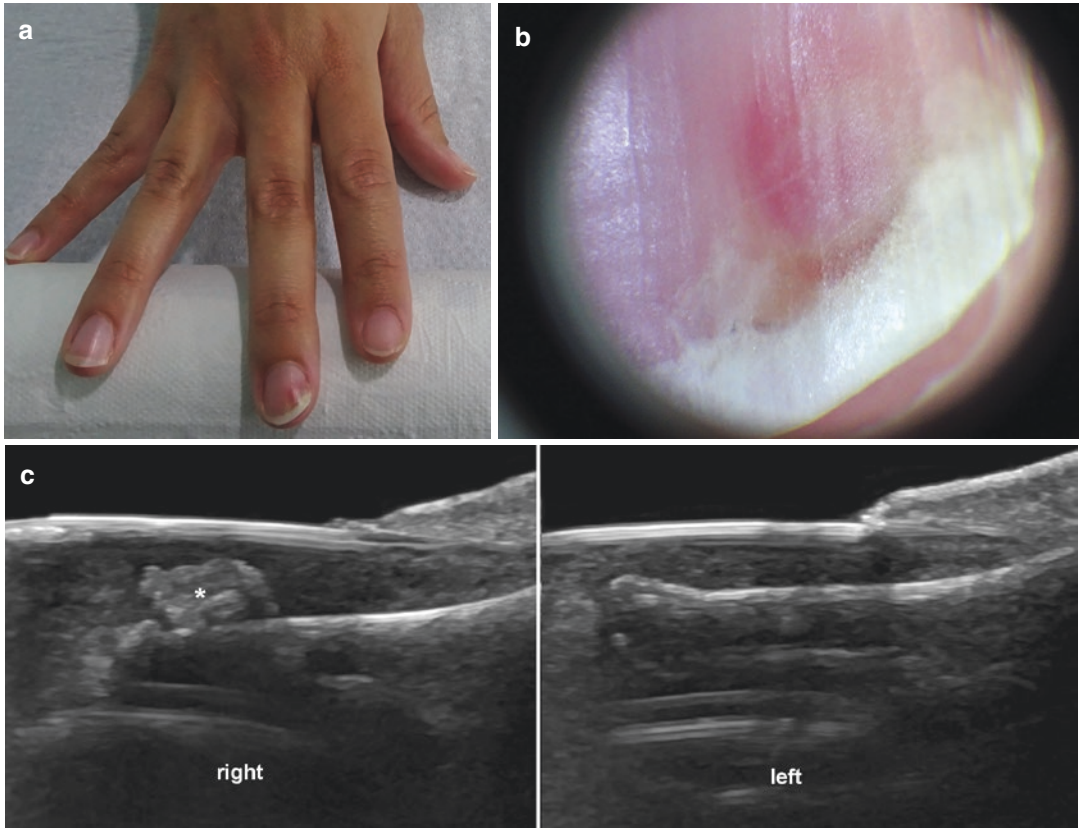


Fig. 18.23 (a–c) Subungual exostosis (right middle finger). (a) Clinical photograph. (b) Dermoscopy. (c) Grayscale ultrasound image (side-by-side; right versus left) presents hyperechoic band (*) protruding into the nail bed at the right side



Fig. 18.24 (a–e) Myxoid cyst (right ring finger). (a) Clinical photograph. (b) Dermoscopy. (c, d and e) Ultrasound images (c and d, longitudinal views; d, transverse view; c, color Doppler, d and e, grayscale; c, at 18 MHz, d and e, at 70 MHz) show oval-shaped, slightly

lobulated structure (*) with mixed echogenicity and posterior acoustic reinforcement artifact (horizontal arrows in d), typically seen in fluid-filled entities. Notice the echoes within this structure in d (o) and the concavity (vertical arrow pointing down) of the nail plate in e

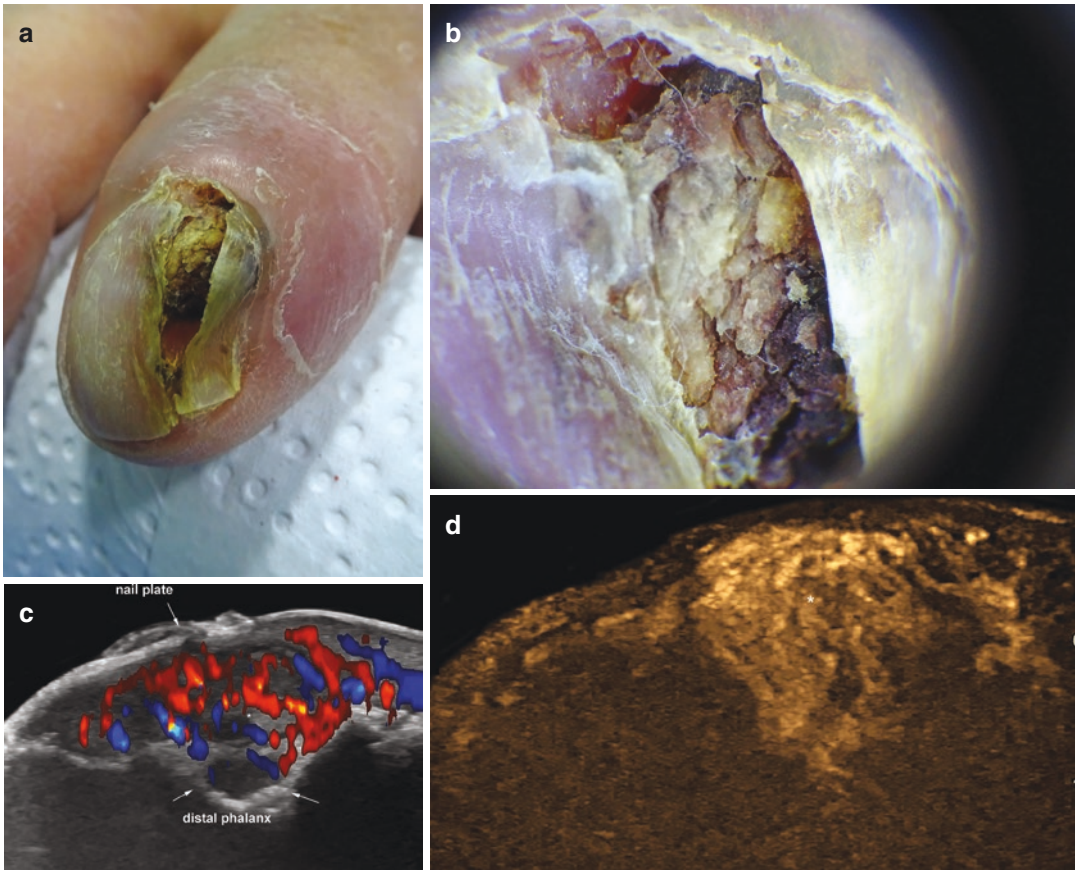


Fig. 18.25 (a–d) Subungual squamous cell carcinoma (right index finger). (a) Clinical photograph. (b) Dermoscopy. (c) Color Doppler and (d) Echoangiography image (B-Flow, General Electric Health Systems, Waukesha, WI) presents an ill-defined hypoechoic and hypervascular

structure (*) that involves the nail bed and erodes the bony margin of the distal phalanx (arrows in c). There are upward displacement and irregular contour of the nail plate (c). Notice the prominent hypervascularity with chaotic distribution (*) in d

melanomas can show as an asymmetric site of hypervascularity without a perceptible mass (Fig. 18.26), or as an ill-defined hypoechoic and hypervascular subungual mass that erodes the nail plate and the bony margin of the distal pha-

lanx [17, 18]. Occasionally, subungual telangiectatic granulomas can mimic melanomas [43]. In congenital melanonychia, there is no subungual hypervascularity [17, 18].

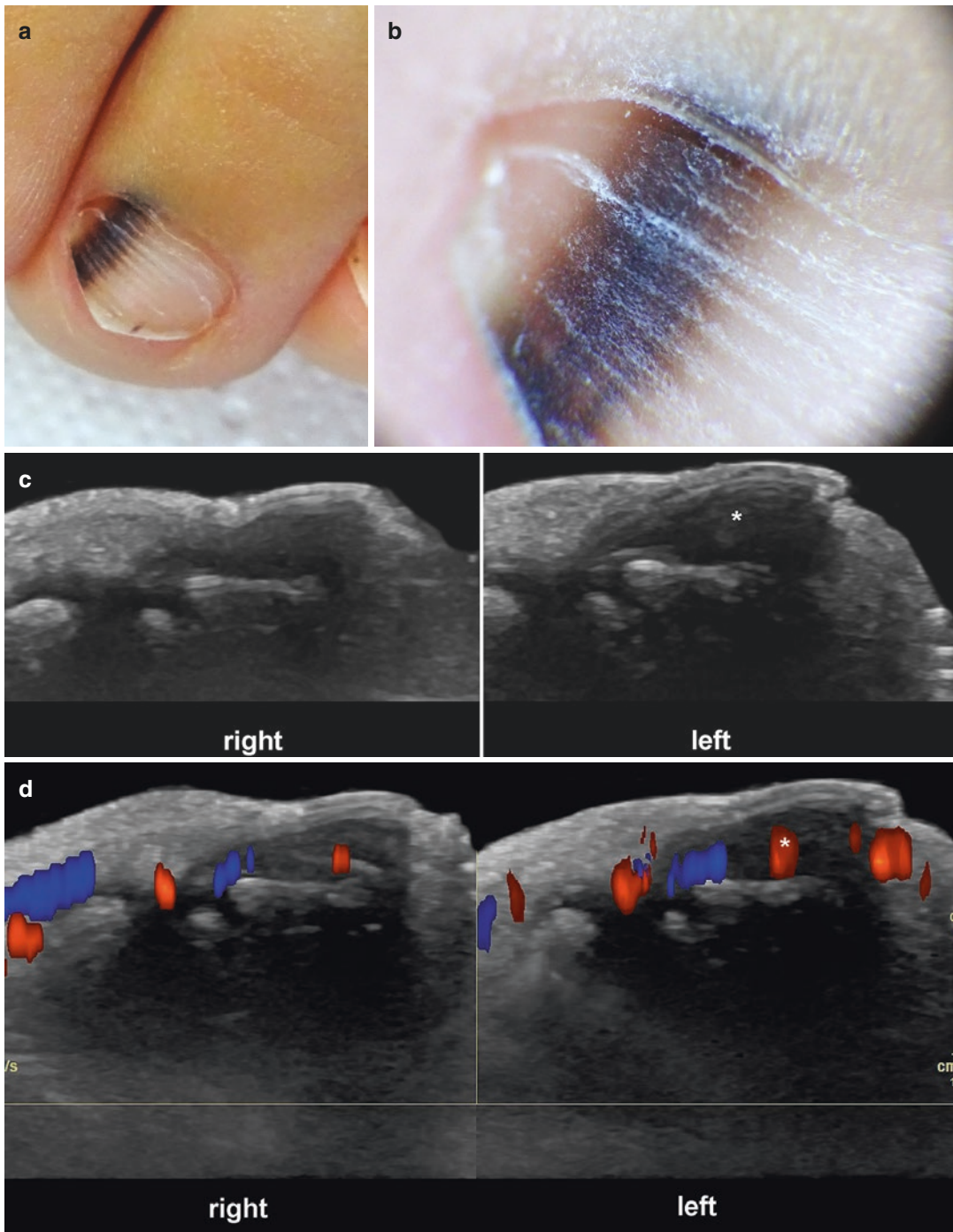


Fig. 18.26 (a–d) Subungual melanoma (left third toe). (a) Clinical image. (b) Dermoscopy. (c) Grayscale and (d) Color Doppler ultrasound (side-by-side comparative views) demonstrate thickening and hypervascularity of

the nail bed with thickening of the nail plate on the left side*. No signs of erosion of the bony margin were detected

References

1. Wortsman X, Jemec GBE. Ultrasound imaging of nails. *Dermatol Clin*. 2006;24(3):323–8. <https://doi.org/10.1016/j.det.2006.03.014>.
2. Aluja Jaramillo F, Quiasúa Mejía DC, Martínez Ordúz HM, González AC. Nail unit ultrasound: a complete guide of the nail diseases. *J Ultrasound*. 2017;20(3):181–92. <https://doi.org/10.1007/s40477-017-0253-6>.
3. Rodríguez-Takeuchi SY, Villota V, Renjifo M. Anatomy and pathology of the nail and subungual space: imaging evaluation of benign lesions. *Clin Imaging*. 2018;52:356–64. <https://doi.org/10.1016/j.clinimag.2018.09.002>.
4. Wortsman X, Wortsman J, Guerrero R, Soto R, Baran R. Anatomical changes in retronychia and onychomadesis detected using ultrasound. *Dermatologic Surg*. 2010;36(10):1615–20. <https://doi.org/10.1111/j.1524-4725.2010.01694.x>.
5. Wortsman X, Wortsman J, Soto R, Saavedra T, Honeyman J. Benign tumors and pseudotumors of the nail: a novel application of sonography. *J Ultrasound Med*. 2010;29(5):803–16.
6. Gutierrez M, Wortsman X, Filippucci E, De Angelis R, Filosa G, Grassi W. High-frequency sonography in the evaluation of psoriasis nail and skin involvement. *J Ultrasound Med*. 2009;28(11):1569–74.
7. Idolazzi L, Zabotti A, Fassio A, et al. The ultrasonographic study of the nail reveals differences in patients affected by inflammatory and degenerative conditions. *Clin Rheumatol*. 2019;38(3):913–20. <https://doi.org/10.1007/s10067-019-04437-0>.
8. Wortsman X, Carreño L, Ferreira-Wortsman C, et al. Ultrasound characteristics of the hair follicles and tracts, sebaceous glands, Montgomery glands, apocrine glands, and arrector pili muscles. *J Ultrasound Med*. 2019;38(8):1995–2004. <https://doi.org/10.1002/jum.14888>.
9. Gungor F, Akyol KC, Eken C, Kesapli M, Beydilli I, Akcimen M. The value of point-of-care ultrasound for detecting nail bed injury in ED. *Am J Emerg Med*. 2016;34(9):1850–4. <https://doi.org/10.1016/j.ajem.2016.06.067>.
10. Wortsman X, Jemec GBE. Role of high-variable frequency ultrasound in preoperative diagnosis of glomus tumors: a pilot study. *Am J Clin Dermatol*. 2009;10(1):23–7.
11. Chiang YP, Hsu CY, Lien WC, Chang YJ. Ultrasonographic appearance of subungual glomus tumors. *J Clin Ultrasound*. 2014;42(6):336–40. <https://doi.org/10.1002/jcu.22138>.
12. Cinotti E, Veronesi G, Labeille B, et al. Imaging technique for the diagnosis of onychomatricoma. *J Eur Acad Dermatol Venereol*. 2018;32(11):1874–8. <https://doi.org/10.1111/jdv.15108>.
13. Fassio A, Giovannini I, Idolazzi L, Zabotti A, Iagnocco A, Sakellariou G. Nail ultrasonography for psoriatic arthritis and psoriasis patients: a systematic literature review. *Clin Rheumatol*. 2020;39(5):1391–404. <https://doi.org/10.1007/s10067-019-04748-2>.
14. Fernández J, Reyes-Baraona F, Wortsman X. Ultrasonographic criteria for diagnosing unilateral and bilateral retronychia. *J Ultrasound Med*. 2018;37(5):1201–9. <https://doi.org/10.1002/jum.14464>.
15. Gutierrez-Manjarrez J, Gutierrez M, Bertolazzi C, Afaro-Rodriguez A, Pineda C. Ultrasound as a useful tool to integrate the clinical assessment of nail involvement in psoriatic arthritis. *Reumatologia*. 2018;56(1):42–4. <https://doi.org/10.5114/reum.2018.74749>.
16. Wortsman X. Common applications of dermatologic sonography. *J Ultrasound Med*. 2012;31(1):97–111. <https://doi.org/10.7863/jum.2012.31.1.97>.
17. Wortsman X. Atlas of dermatologic ultrasound. In: Wortsman X, editor. New York: Springer; 2018. <https://doi.org/10.1007/978-3-319-89614-4>.
18. Wortsman X, Jemec GBE. Dermatologic ultrasound with clinical and histologic correlations. In: Wortsman X, Jemec GBE, editors. New York: Springer; 2013. <https://doi.org/10.1007/978-1-4614-7184-4>.
19. Wortsman X, Alfageme F, Roustan G, et al. Proposal for an assessment training program in dermatologic ultrasound by the DERMUS Group. *J Ultrasound Med*. 2016;35(11):2305–9. <https://doi.org/10.7863/ultra.15.10068>.
20. Kromann CB, Wortsman X, Jemec GBE. High-frequency ultrasound of the nail. In: Agache's measuring the skin: non-invasive investigations, physiology, normal constants: second edition. Springer International Publishing; 2017. p. 891–6. https://doi.org/10.1007/978-3-319-32383-1_123.
21. Wortsman X. Sonography of dermatologic emergencies. *J Ultrasound Med*. 2017;36(9):1905–14. <https://doi.org/10.1002/jum.14211>.
22. Litaïem N, Drissi H, Zeglouï F, Khachemoune A. Retronychia of the toenails: a review with emphasis on pathogenesis, new diagnostic and management trends. *Arch Dermatol Res*. 2019;311(7):505–12. <https://doi.org/10.1007/s00403-019-01925-w>.
23. Wortsman X, Calderon P, Baran R. Finger retronychias detected early by 3D ultrasound examination. *J Eur Acad Dermatol Venereol*. 2012;26(2):254–6. <https://doi.org/10.1111/j.1468-3083.2011.04068.x>.
24. Pizarro M, Pieressa N, Wortsman X. Posttraumatic retronychia of the foot with clinical and ultrasound correlation. *J Am Podiatr Med Assoc*. 2017;107(3):253–6.
25. Wortsman X, Gutierrez M, Saavedra T, Honeyman J. The role of ultrasound in rheumatic skin and nail lesions: a multi-specialist approach. *Clin Rheumatol*. 2011;30(6):739–48. <https://doi.org/10.1007/s10067-010-1623-z>.
26. Idolazzi L, Gisondi P, Fassio A, et al. Ultrasonography of the nail unit reveals quantitative and qualitative alterations in patients with psoriasis and psoriatic arthritis. *Med Ultrason*. 2018;20(2):177–84. <https://doi.org/10.11152/mu-1327>.

27. Krajewska-Włodarczyk M, Owczarczyk-Saczonek A, Placek W, Wojtkiewicz M, Wiktorowicz A, Wojtkiewicz J. Ultrasound assessment of changes in nails in psoriasis and psoriatic arthritis. *Biomed Res Int.* 2018;2018:8251097. <https://doi.org/10.1155/2018/8251097>.
28. Mendonça JA, Aydın SZ, D'Agostino MA. The use of ultrasonography in the diagnosis of nail disease among patients with psoriasis and psoriatic arthritis: a systematic review. *Adv Rheumatol (London, England).* 2019;59(1):41. <https://doi.org/10.1186/s42358-019-0081-9>.
29. Moreno M, Lisbona MP, Gallardo F, et al. Ultrasound assessment of psoriatic onychopathy: a cross-sectional study comparing psoriatic onychopathy with onychomycosis. *Acta Derm Venereol.* 2019;99(2):164–9. <https://doi.org/10.2340/00015555-3060>.
30. Moya Alvarado P, Roé Crespo E, Muñoz-Garza FZ, et al. Subclinical enthesopathy of extensor digitorum tendon is highly prevalent and associated with clinical and ultrasound alterations of the adjacent finger-nails in patients with psoriatic disease. *J Eur Acad Dermatol Venereol.* 2018;32(10):1728–36. <https://doi.org/10.1111/jdv.15035>.
31. Ureyen SB, Kara RO, Erturk Z, Yaldiz M. The microvascular and morphostructural changes of nails in psoriatic patients with nail disease; a link between ultrasound and videocapillaroscopy findings in the nailfold. *Med Ultrason.* 2018;20(2):185–91. <https://doi.org/10.11152/mu-1274>.
32. Zabotti A, Errichetti E, Zuliani F, et al. Early psoriatic arthritis versus early seronegative rheumatoid arthritis: role of dermoscopy combined with ultrasonography for differential diagnosis. *J Rheumatol.* 2018;45(5):648–54. <https://doi.org/10.3899/jrheum.170962>.
33. Choi JW, Kim BR, Seo E, Youn SW. Identification of nail features associated with psoriasis severity. *J Dermatol.* 2017;44(2):147–53. <https://doi.org/10.1111/1346-8138.13565>.
34. Rigopoulos D, Baran R, Chiheb S, et al. Recommendations for the definition, evaluation, and treatment of nail psoriasis in adult patients with no or mild skin psoriasis: a dermatologist and nail expert group consensus. *J Am Acad Dermatol.* 2019;81(1):228–40. <https://doi.org/10.1016/j.jaad.2019.01.072>.
35. Chaowattanapanit S, Pattanaprichakul P, Leeyaphan C, et al. Coexistence of fungal infections in psoriatic nails and their correlation with severity of nail psoriasis. *Indian Dermatol Online J.* 2018;9(5):314–7. https://doi.org/10.4103/idoj.IDOJ_192_17.
36. Yamaoka T, Hayashi M, Tani M, Katayama I. Value of ultrasonography findings for nail psoriasis before and after adalimumab administration. *Clin Exp Dermatol.* 2017;42(2):201–3. <https://doi.org/10.1111/ced.12980>.
37. Schioppo T, Orenti A, Boracchi P, De Lucia O, Murgo A, Ingegnoli F. Evidence of macro- and micro-angiopathy in scleroderma: an integrated approach combining 22-MHz power Doppler ultrasonography and video-capillaroscopy. *Microvasc Res.* 2019;122:125–30. <https://doi.org/10.1016/j.mvr.2018.07.001>.
38. Wortsman X, Sazunic I, GBE J. Sonography of plantar warts: role in diagnosis and treatment. *J Ultrasound Med.* 2009;28(6):787–93. <https://doi.org/10.7863/jum.2009.28.6.787>.
39. Wortsman X, Jemec GBE, Sazunic I. Anatomical detection of inflammatory changes associated with plantar warts by ultrasound. *Dermatology.* 2010;220(3):213–7. <https://doi.org/10.1159/000275607>.
40. Lee JK, Kim TS, Kim DW, Han SH. Multiple glomus tumours in multidigit nail bed. *Handchirurgie Mikrochirurgie Plast Chir.* 2017;49(5):321–5. <https://doi.org/10.1055/s-0043-115115>.
41. Soto R, Wortsman X, Corredoira Y. Onychomatricoma: clinical and sonographic findings. *Arch Dermatol.* 2009;145(12):1461–2. <https://doi.org/10.1001/archdermatol.2009.312>.
42. Wortsman X, Wortsman J. Clinical usefulness of variable-frequency ultrasound in localized lesions of the skin. *J Am Acad Dermatol.* 2010;62(2):247–56. <https://doi.org/10.1016/j.jaad.2009.06.016>.
43. Silva-Feistner M, Ortiz E, Alvarez-Vélez S, Wortsman X. Amelanotic subungual melanoma mimicking telangiectatic granuloma: clinical, histologic, and radiologic correlations. *Actas Dermosifiliogr.* 2017;108(8):785–7. <https://doi.org/10.1016/j.ad.2017.03.008>.